Inductive measurements of UPt_3 in the superconducting state

P. J. C. Signore, B. Andraka, and M. W. Meisel*
Department of Physics and the Center for Ultralow Temperature Research, University of Florida, 215 Williamson Hall, P.O. Box 118440, Gainesville, Florida 32611-8440

S. E. Brown
Department of Physics, University of California at Los Angeles, Los Angeles, California 90024

Z. Fisk,† A. L. Giorgi, and J. L. Smith
Los Alamos National Laboratory, Los Alamos, New Mexico 87545

F. Gross-Alltag and E. A. Schuberth
Walther Meissner Institut, D-85748 Garching, Germany

A. A. Menovsky
Natuurkundig Laboratorium der Universiteit van Amsterdam, Valckenierstraat 65, 1018 XE Amsterdam, The Netherlands
(Received 27 December 1994)

The inductive response of several UPt_3 samples obtained from four different materials-fabrication groups has been measured from 50 to 700 mK at frequencies varying between 32 Hz and 33 MHz. The temperature dependence of the penetration depth, $\lambda(T)$, is presented for each sample. The low-frequency (≤ 4.7 kHz) data suggest a linear temperature dependence of $\lambda(T/T_c \leq 0.5)$ for the samples possessing a double feature near the superconducting transition temperature T_c. We have verified that this double feature present in $\lambda(T)$ for some of the samples corresponds to the double jump observed in the specific heat. On the other hand, $\lambda(T/T_c \leq 0.5)$ is found to have a quadratic temperature dependence for unannealed specimens which exhibit only a single transition at T_c. The linear temperature dependence of $\lambda(T)$ is consistent with the presence of line nodes in the basal plane, while the quadratic dependence found for other samples suggests that impurity scattering dominates in these specimens. The double transition in $\lambda(T)$ has been studied in magnetic fields up to 1.6 T, and the resulting phase diagram is consistent with the one constructed from thermodynamical measurements. The high-frequency (≥ 3 MHz) data suggest $\lambda(T/T_c \leq 0.5) \propto T^{\eta}$, where $2 \leq \eta \leq 4$. The possible origins of the frequency dependence of $\lambda(T)$ are discussed, as well as the effect of the surface quality on η.

I. INTRODUCTION

The discovery of superconductivity in the heavy-fermion system UPt_3 (Ref. 1) sparked great excitement for the study of this material both experimentally[2] and theoretically.[3] For the past decade, several experimental findings have established various unusual phenomena related to the superconducting state of UPt_3. For example, specific-heat measurements have revealed a double jump near the superconducting transition temperature, T_c,[4] and different techniques probing the magnetic-field–temperature-pressure dependencies of T_c have mapped a multiple-phase diagram.[5–10] Moreover, the temperature dependences of various transport and thermodynamic properties below T_c do not fit the behavior expected for BCS-like superconductors with a finite energy gap.[11–16]

The primary motivations driving this work were threefold. The first objective was to establish the temperature dependence of the penetration depth, $\lambda(T)$, deep into the superconducting state. This quantity is related to the superconducting electron density, $n_s(T)$, by the expression

$$\lambda(T) = \left[\frac{m^* c^2}{4\pi e^2} \frac{1}{n_s(T)} \right]^{1/2} . \quad (1)$$

The temperature dependence of the superconducting electron density is determined by the energy gap structure. For example, if the energy gap is finite around the Fermi surface, then the quasiparticles will be thermally activated across the gap, consequently $n_s(T)$, as well as $\lambda(T)$, will assume exponential forms. On the other hand, if the energy gap has nodes, $n_s(T)$ and $\lambda(T)$ will follow power laws in the $T/T_c \rightarrow 0$ limit.[14]

Several measurements of $\lambda(T)$ in UPt_3 have been reported.[14,17–24] In each case, the data followed a power law

$$\lambda(T) - \lambda(0) \propto T^{\eta} , \quad (2)$$

where the range of η ($1 \leq \eta \leq 4$) may be due to crystalline anisotropy and to differences in both the measuring method and fabrication protocols of the samples. The above measurements were performed above $T/T_c \approx 0.1$

0163-1829/95/52(6)/4446(16)/$06.00

(50 mK), so a limited range of temperature was available for fitting power laws. In this work, the fitting of the power laws was performed for temperature between $T/T_c \approx 0.1$ ($T \approx 50$ mK) and $T/T_c \approx 0.5$ ($T \approx 260$ mK). Consequently, these results reflect *trends* in $\lambda(T)$ which can be compared from sample to sample. However, we cannot comment on the true $T \rightarrow 0$ limit.

Measurements of $\lambda(T)$ have been a powerful tool in the study of numerous superconductors. For example, the linear temperature dependence of $\lambda(T)$ in $YBa_2Cu_3O_{7-\delta}$ single crystals has been taken as evidence for non-*s*-wave BCS superconductivity.[25] Similar measurements performed on Zn-doped $YBa_2Cu_3O_{7-\delta}$ crystals[26] and on thin films[27] lead to quadratic temperature dependences, suggesting that, in this system, sample composition and geometry play an important role in the observed temperature dependence of $\lambda(T)$.

Our second objective was to study the possible frequency dependence of the penetration depth. Earlier reports of inductive measurements for $T/T_c \leq 0.5$ revealed a discrepancy between data taken at low frequencies (dc–317 Hz) (Refs. 14, 18, and 23) and those obtained from a resonant technique at radio frequencies (3–47 MHz).[19,20,23] A frequency dependence of $\lambda(T)$ is not expected for superconductors possessing finite energy gaps around their Fermi surfaces as long as the probing frequency is much lower than the gap energy (≈ 20 GHz in UPt_3). On the other hand, if the gap has nodes, then a finite frequency may alter $\lambda(T)$. This issue has been discussed by Putikka, Hirschfeld, and Wölfle[28] and Hirschfeld *et al.*[29] who calculated the temperature dependence of $\lambda(T)$ for the E_{1g} state and for various frequencies. Their results will be discussed further in relation to our work. In order to determine whether the experimentally observed frequency dependence was related to intrinsic properties of the superconducting state, experimental techniques and/or details of the sample fabrication histories, we have measured $\lambda(T)$ using inductive techniques over a wide range of frequencies (32 Hz to 33 MHz) with the same samples.

Our third goal was to investigate the effects of surface roughness on our measurements. As mentioned above, one of the factors that has made the overall interpretation of the data on UPt_3 difficult is the sensitivity of the results to sample history. For instance, not all samples exhibit double jumps in the specific heat near T_c. Other heavy-fermion systems are known to suffer from similar materials preparation problems. For example, measurements on specimens of UBe_{13} have shown conflicting results regarding a possible magnetic transition around 10 K (Refs. 30 and 31) and the crystalline anisotropy of $H_{c2}(T/T_c \rightarrow 1)$.[32] Consequently, crystal growth techniques and sample preparation (annealing, etching, polishing, cutting, etc.) become crucial issues in this field.

The details of the experimental techniques are presented in the following section. In addition, the fabrication protocols for all of our samples are described. In the third section, the results of our measurements are given. After a detailed discussion of our observations in Sec. IV, we conclude our work.

II. EXPERIMENTAL DETAILS

Using a variety of samples whose histories are given in the last subsection, we have measured $\lambda(T)$ using two different techniques, which are described in detail in the following subsections. A standard mutual inductance measurement was used for frequencies between 32 Hz and 4.7 kHz, and a resonant technique was utilized for frequencies between 3 MHz and 33 MHz. For both methods, the samples were GE varnished to two or four copper wires which were passed through the coils and then bolted to the mixing chamber of a dilution refrigerator. Studies of $\lambda(T)$ in a dc magnetic field were performed by mounting the mutual inductance coil, the sample, and a thermometer to the end of a copper cold finger so as to place them at the center of a superconducting solenoid (0–8 T) located in the main liquid-helium bath of the dewar.

Unless otherwise stated, all the data presented in this paper have been taken under nominal zero-field-cooled conditions. More specifically, the samples were first cooled to the minimum temperature, $T_{\min}$, of the dilution refrigerator ($T_{\min} \approx 50$ mK) in the presence of the Earth's field before the probing ac field was applied, and subsequently the temperature was increased. The temperature, determined by a germanium resistor located on the mixing chamber, was carefully controlled so that large deviations and oscillations across the set point did not occur. Each point was taken after the temperature had come to equilibrium, which took place after approximately 3 min. Any possible temperature-dependent background arising from the coil and the thermal anchoring copper wires was independently measured when the specimens were not present. For all measurements, the background contributed less than 10% of the observed changes. This parasitic contribution was fitted to an analytic expression which was used to correct the total signal.

A. Mutual inductance measurements

We have used standard, well-known mutual inductance techniques to measure the temperature dependence of the penetration depth. The details of the various coils and their geometries are described by Signore.[32] An important feature of our measurements is the use of two PAR 124A lock-in amplifiers to detect the real and imaginary components of the signal. In all experiments, the probing ac magnetic field, B_{ac} was less than approximately 10 μT. The remainder of this subsection discusses the relationship between the detected signal and the penetration depth of the sample. This relationship is supported by our control experiments on Al and Zn. These results are discussed at the end of this subsection.

When a specimen is located in one of the two counterwound pick-up coils, the signal detected by the lock-in amplifiers corresponds to the difference between the voltage due to $d\Phi/dt$ (Φ is the magnetic flux) in the two pick-up coils, given by

$$V = 2\pi \frac{d}{dt} \left[\int B(r) r dr \right] - i\omega \pi r_s^2 B_{ac} , \quad (3)$$

where r_s is the radius of the sample, $\omega=2\pi f$, and f is the probing frequency. In addition, we have assumed a circular sample cross section and $B(r,\theta,z)=B(r)$. We may define the magnetic susceptibility χ by

$$\frac{2\pi}{\pi r_s^2}\int B(r)rdr=\mu_0(1+\chi)H_{\rm ac} , \tag{4}$$

where $B_{\rm ac}=\mu_0 H_{\rm ac}$ with μ_0 the permeability of free space. Substituting Eq. (4) into Eq. (3) yields

$$V=i\omega\pi r_s^2 B_{\rm ac}\chi . \tag{5}$$

In other words, from Eq. (5) the detected voltage is directly proportional to the magnetic susceptibility of the sample.

For a normal metal, we know from Maxwell's equations that the field inside the sample must satisfy

$$\nabla^2\mathbf{B}+K^2\mathbf{B}=0 , \tag{6}$$

where $K^2=i4\pi\sigma_n\omega/c^2$ and where σ_n is the normal metal conductivity. For a cylindrical sample of radius r_s and with the field parallel to its axis, Eq. (6) can be solved explicitly, giving the textbook result

$$B(r)=B_{\rm ac}J_0(Kr)/J_0(Kr_s) , \tag{7}$$

where J_0 is the zeroth-order Bessel function.[33]

The magnetic susceptibility, $\chi=\chi'+i\chi''$, can then be calculated by substituting Eq. (7) for $B(r)$ into Eq. (4). By measuring both the in-phase component of the output signal and its quadrature, we obtain χ' and χ'' independently. Maxwell and Strongin[34] have shown that if Eq. (7) is used in Eq. (4) then both χ' and χ'' are essentially zero for $r_s/\delta\leq 0.5$, where r_s is the radius of the sample and δ is the normal-state skin depth given by

$$\delta(T)=[2/\mu\sigma_n(T)\omega]^{1/2} . \tag{8}$$

Given this analysis, we do not expect any significant signal above T_c for our sample geometries and experimental conditions. For instance, consider our sample no. 1 with $r_s\approx 0.20$ mm (Table I) and $\delta(T_c, 317\ {\rm Hz}) = 2.7$ mm, then $r_s/\delta\approx 0.075 \ll 0.5$.

Below T_c, Eqs. (3)–(7) still hold, but σ_n is replaced by $\sigma_s=\sigma_1+i\sigma_2$, where σ_1 and σ_2 are the real and imaginary parts of conductivity, respectively. Just below T_c, both components of the complex conductivity contribute to χ' and χ''. This effect makes the analysis of the data around T_c difficult. In fact, there exists a controversy about the microscopic mechanism responsible for the peak in χ'' in the vicinity of T_c observed in other materials.[35,36] At lower temperatures, σ_1 and χ'' to zero and the field inside the sample takes the form

$$B(r)=B_a e^{-(r_s-r)/\lambda} , \tag{9}$$

where λ is given by

$$\lambda^2=c^2/4\pi\sigma_2\omega . \tag{10}$$

Substituting the field distribution given by Eq. (9) into Eq. (4), we obtain

$$\chi'(T)=-1+\frac{2\lambda(T)}{r_s} , \tag{11}$$

where the temperature dependence of $\chi'(T)$ and $\lambda(T)$ have been explicitly noted. From Eq. (11), we see that the temperature dependence of the penetration depth can be established by measuring $\chi'(T)$. The uncertainties in the exact values of $B_{\rm ac}$, the gain of the lock-in amplifier, and more importantly r_s, keep us from extracting precise absolute values for $\lambda(T)$. Consequently, our mutual inductance results only enable us to measure $\lambda(T)$ in arbitrary units.

In order to check our technique, we have measured a

TABLE I. Characteristics of the four samples investigated in this study. The last two columns list the exponents, η, as defined by Eq. (2). D is the demagnetization factor as estimated from Ref. 45.

Sample	Geometry	Dimensions and D	Treatment	References	η at low frequencies	η at rf frequencies
No. 1	Single crystals, needles c axis ∥ long axis	$r_s=0.2$ mm length = 3 mm $D\approx 0.035$	Annealed at 950°C for 100 h in Ta foil, etched in HCl:HNO_3 (3:1), polished (0.3 μm diamond) film)	23,24,32	$f=317$ Hz unpolished: 1±0.1 $f=317$ Hz polished: 1±0.1	$f=3$, 16 MHz unpolished: 2.6±0.2 $f=6$ MHz polished: 3.7±0.2
No. 2	Single crystal, cylinder c axis ∥ long axis	$r_s=1.25$ mm length = 5 mm $D\approx 0.175$	Not annealed, polished	14,17,32, 47–49	$f=417$ Hz: 2±0.2	$f=5.6$ MHz: 2.4±0.2
No. 3	Single crystal parallelepiped c axis ∥ 3.7 side	3.7×0.6×0.6 mm^3 $D\approx 0.035$	Spark erosion cut, not annealed, not polished	22,32 50–53	$f=317$ Hz: 2±0.1	$f=15$ MHz: 2±0.1
No. 4	Polycrystal, cylinder	$r_s=1$ mm length = 5 mm $D\approx 0.135$	Annealed at 950°C for 90 h	4,20,32	$f=317$ Hz: $T<200$ mK: 1±0.1	$f=14$ MHz: 4

number of well-characterized superconductors such as Al and Zn. Figure 1 shows $\chi'(T)$ for a cylindrical specimen ($l=2.5$ mm, $r_s=0.2$ mm) of $6N$ purity aluminum.[37] The onset transition temperature was observed at 1.180 K which is in excellent agreement with earlier work on aluminum by other groups.[38,39] An important aspect of the data is that $\chi'(T)$ appeared to reach its minimum value just below T_c, i.e., $\chi'(T)$ was flat, within our experimental resolution, from 1.1 K to $T_{\min}$. This result can be explained by an exponentially decaying $\lambda(T)$, with changes in λ for $T<1.1$ K smaller than our experimental resolution. The data on zinc showed similar steplike behavior.[32]

B. Resonant technique

Tunnel diode resonating circuits have been used to study $\lambda(T)$ of various superconductors for a number of years.[39,40] The principle works on the basis of a small bias voltage (≈ 150 mV) being applied across a tunnel diode[41] to keep it within its negative resistance region. The diode then generates a small oscillating current (~ 100 μA) through a tank circuit connected in series with it. The specimen to be studied is placed inside an inductor, L, of the circuit. A change in either the penetration depth for $T<T_c$, or the skin depth for $T>T_c$, causes a change in inductance which in turn results in a shift in the resonant frequency. It can be shown[42] that the change in frequency of the oscillator is given by

$$\frac{\Delta f}{f_0}=-\frac{\Delta L}{2L_0}\left[1-\frac{2}{Q^2}\right]-\frac{\Delta R}{R}\left[\frac{1}{Q^2}\right], \tag{12}$$

where R is the resistance of the tank circuit, $Q=2\pi fL/R$, $\Delta f=f(T_{\min})-f(T)$, $f_0=f(T_{\min})$, $\Delta L=L(T_{\min})-L(T)$, and $L_0=L(T_{\min})$. Thus if Q is large enough, the relative change of frequency is simply given by

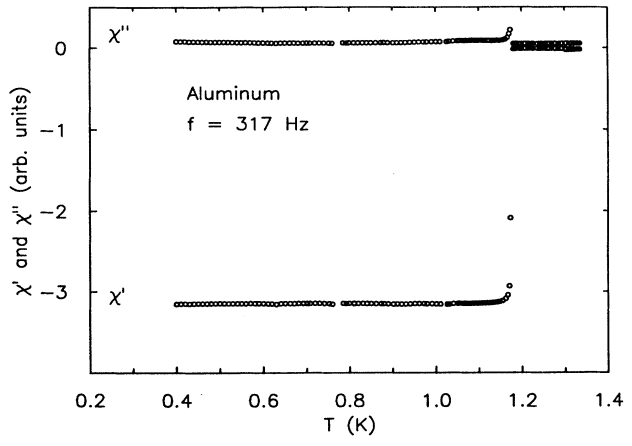

FIG. 1. The real part of the susceptibility, $\chi'(T)$, as a function of temperature for Al at 317 Hz. The onset transition is 1.180 K in good agreement with the 10-MHz data (Fig. 2). Within our experimental uncertainties, $\chi'(T)$ was flat below 1.1 K.

$$\frac{\Delta f}{f_0}=-\frac{\Delta L}{2L_0}. \tag{13}$$

Tedrow, Faraci, and Meservey[39] measured the Q of tunnel diode oscillating (TDO) circuits similar to the one used here, and found that if the Q is large enough (>100) to allow oscillations, then it is large enough to make the terms in $1/Q^2$ in Eq. (12) negligible, so that Eq. (13) can indeed be used. We qualitatively verified this assertion by performing TDO measurements on Cu with various size inductors and samples, and found that for small L (low Q) the circuit did not oscillate, but for larger L (high Q) oscillations were stable. Equation (13) can also be written as

$$\frac{\Delta f}{f_0}=\frac{\pi r_s \Delta\Lambda}{A}, \tag{14}$$

where r_s is the radius of the sample, A is the cross-sectional area between the coil and the sample, and Λ is either the skin depth δ when $T>T_c$ as defined in Eq. (8) or the penetration depth λ for $T<T_c$ as defined in Eq. (10). Consequently, the experiment consists of monitoring the frequency as a function of temperature.

The disadvantage of this technique, compared to a mutual inductance measurement, is its inability to measure the resistive contribution. On the other hand, one advantage comes from the fact that, in the normal state, $\Delta f/f$ is proportional to $\Delta\delta(T)$. If the resistivity of the sample just above T_c is known, then one can use the normal-state data to calibrate the coil and estimate absolute values for $\lambda(T)$. This procedure was done in our earlier work where we reported $\lambda(T\rightarrow 0)=2.1\pm 0.2$ μm for sample no. 1.[23] Although this value is consistent with some published results,[14,43] it is larger than the value reported by other groups.[19,21]

Several coils, with inductances on the order of 1 μH, were fabricated in order to maximize the packing factor for the differently sized samples. This technique enables us to achieve frequency stability on the order of 5 parts in 10^6 or better. The radio frequency field, $\mathbf{B}_{\rm rf}$, generated inside the inductor was always less than 10 μT.

To check our method, we have performed several runs on Al and Zn. The data for a cylindrical specimen ($l=6.3$ mm, $r_s=0.5$ mm) of $6N$ purity Al (Ref. 37) is shown in Fig. 2. The onset transition temperature was observed at 1.175 K, in excellent agreement with the results of other groups[38,39] and with T_c observed in our low-frequency measurements (Fig. 1), indicating that there was negligible self-heating caused by the higher frequencies. The data could be fitted very well to the BCS temperature dependence for a nonlocal superconductor, namely

$$\lambda(T)=\lambda(0)\left[\frac{\Delta(t)}{\Delta(0)}\tanh\left[\frac{3.53\Delta(t)}{4t\Delta(0)}\right]\right]^{-1/3}, \tag{15}$$

where $\Delta(t)$ is the BCS energy gap function, $t=T/T_c$, and we have assumed $\lambda(0)=520$ Å which is the estimated value for aluminum.[44]

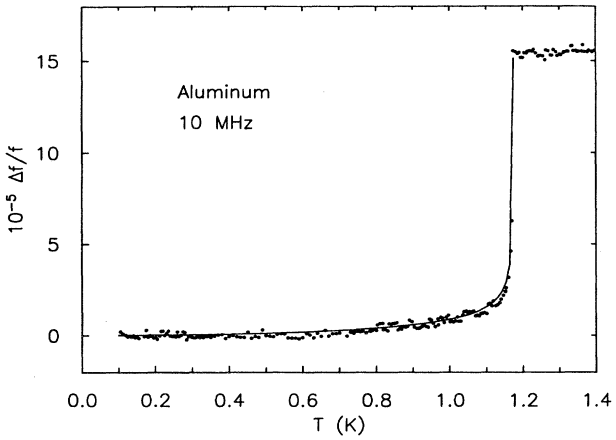

FIG. 2. The relative change in frequency, $\Delta f/f=[f(T_{\min})-f(T)/f(T_{\min})]$, as a function of temperature for Al at 10 MHz. The solid line is a nonlinear least-squares fit to a BCS temperature dependence given in the text. The transition temperature is 1.175 K in good agreement with the 317 Hz data (Fig. 1).

C. Sample history

During the course of this work, a number of specimens have been investigated, and the results acquired from four of the samples are presented in this paper. Since the data from the other specimens do not add any new information to our discussion here, they are presented elsewhere.[32] Table I summarizes the properties of the four samples described in this paper. Additional information about each sample is given in the following paragraphs of this subsection.

Sample No. 1 was comprised of single crystals which were grown by Fisk at Los Alamos National Laboratory using a Bi flux from which they were quenched. These needles were first studied inductively before *any* treatment was performed on them. These preliminary results showed a sharp diamagnetic response around 1.3 K in addition to the UPt_3 superconducting transition around 0.5 K. Although the exact nature and origin of the 1.3-K anomaly are unknown, we suspect a BiPt superconducting surface phase may have been present.[46] The needles were then annealed (100 h at 950 °C wrapped in Ta foil), etched [about 1 min in HCl:HNO_3 (3:1)], and subsequently remeasured.[23] After etching, the 1.3-K anomaly was no longer observable.[32] These crystals were further studied after polishing their surface with very fine paper of 0.3 μm grading. Figure 3 shows three scanning electron microscope (SEM) pictures of the surfaces at different stages of the treatment where the characteristic length scale of the surface imperfections went from about 2 to 0.5 μm. In addition to our inductive measurements on this sample, we have measured its resistivity, where the onset of the transition was 530 mK,[23] and its specific heat which is presented in the next section.

The first penetration depth measurement reported on UPt_3 was performed on single-crystal No. 2 using a dc method.[18] The observed T^2 dependence of $\lambda(T)$ was later attributed to the presence of impurities.[14] The specific heat of this sample was also measured down to 10 mK (sample no. 1 of Schuberth *et al.*[47]) where the data showed an interesting upturn around 18 mK. On the other hand, sound velocity measurements on a different UPt_3 sample down to 5 mK did not show any manifestation of this anomaly.[15] Earlier specific-heat measurements on our sample No. 2 showed no signs of a double jump around T_c.[48] We were interested in this particular sample to check if we could reproduce the T^2 dependence with our low-frequency mutual inductance technique and thereby demonstrate the equivalence between our method and the dc measurements.[14,18,47] This single crystal was grown by electron beam melting in an ultrahigh-vacuum zone refining furnace using uranium that was depleted to less than 100 ppm ^{235}U. The surfaces were polished,[49] and SEM pictures of the surface are shown in Fig. 4. The characteristic length scale of the surface imperfections were less than 1 μm except for a number of scattered "pin holes" shown in Fig. 4(b). These local defects were 10 to 20 μm in diameter and appeared to be at least 10 μm

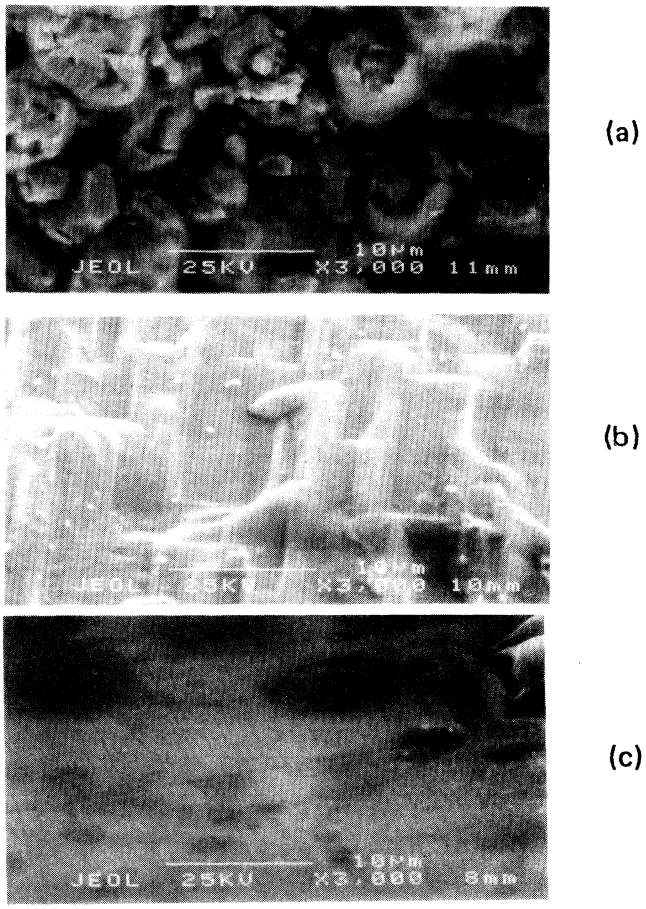

FIG. 3. SEM pictures ($\times$3000 magnification) of the surface of single crystal no. 1 (Table I). (a) As grown; (b) annealed, etched, unpolished; (c) annealed, etched, polished. The length scale of the imperfections improve from about 2 μm to less than 0.5 μm.

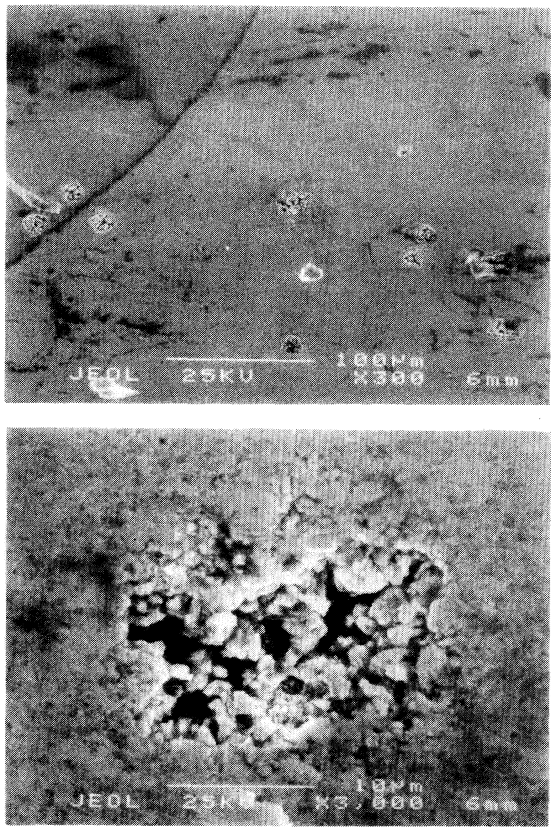

FIG. 4. 4 SEM pictures of the surface of single crystal no. 2 (Table I). (a) $\times 300$ magnification, the length scale of the imperfections is less than 2 μm, except to a few cracks (upper left corner) and scattered "pin holes" occupying less than 5% of the total surface area. (b) $\times 3000$ magnification, focusing on one of the "pin holes."

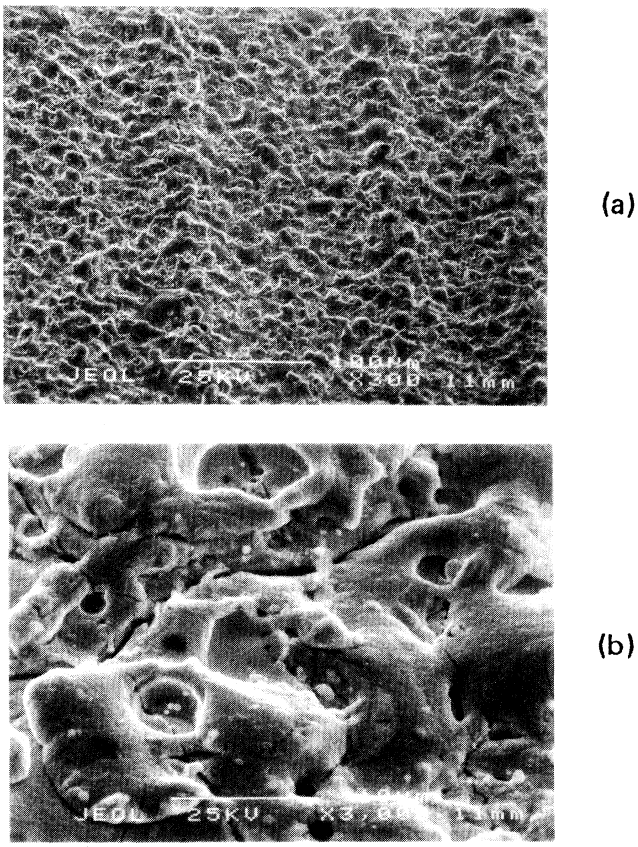

FIG. 5. SEM pictures of a specimen originating from the same batch as sample no. 3 (Table I). (a) $\times 300$ magnification. (b) $\times 3000$ magnification. Imperfections possessing a length scale between 1 and 10 μm cover the entire surface.

deep. They covered about 5% of the total surface of the sample. This sample was not annealed.

Sample no. 3 was spark erosion cut from a large single-crystal grown using a modified Czochralski tri-arc method[50] and was unannealed.[51] Other specimens originating from the same crystal were annealed and showed a pronounced increase in the double jump in the specific-heat data without changing T_c.[22,51–53] The surface was not treated after the spark erosion process, and SEM pictures of the surface of a sample originating from the same batch as no. 3 are shown in Fig. 5. The entire surface is covered with imperfections of size ranging from 1 to 10 μm.

Sample no. 4 was the polycrystal in which the double peak in the specific heat was first reported as an intrinsic feature of UPt_3.[4] The results on the rf penetration depth have already been published,[20] but the low-frequency work has not. We were also interested in this sample to check if the double peak in specific heat corresponds to any features in our inductive measurements. Our sample was cut from a large arc-melted polycrystalline ingot, and the surface was not further characterized.

III. RESULTS

A. Mutual inductance results

As mentioned earlier, the mutual inductance data are given in arbitrary units. However, all the results presented in this paper were taken with the same excitation field, B_{ac}, and lock-in amplifier gain; furthermore, the raw data signals were divided by the probing frequency. Consequently, the arbitrary units reported for all samples possess the same scale, with differences in the signal sizes arising from variations in specimen geometry and from intrinsic properties of the material. In addition, $\chi'(T)$ and $\chi''(T)$ of a given sample share the same units, with the exception of Fig. 6 (see next paragraph). For the three single crystals, sample nos. 1, 2, and 3, the probing ac field, B_{ac}, was oriented parallel to the c axis of the crystal.

The data for sample no. 1 between 400 and 600 mK are shown in Fig. 6. The crosses correspond to the "as-grown" sample. The circles represent the data taken after annealing and etching, but before polishing. The diamonds show the data taken after annealing, etching, and polishing. The total change in signal across T_c for the raw data was different for each set, reflecting the fact that

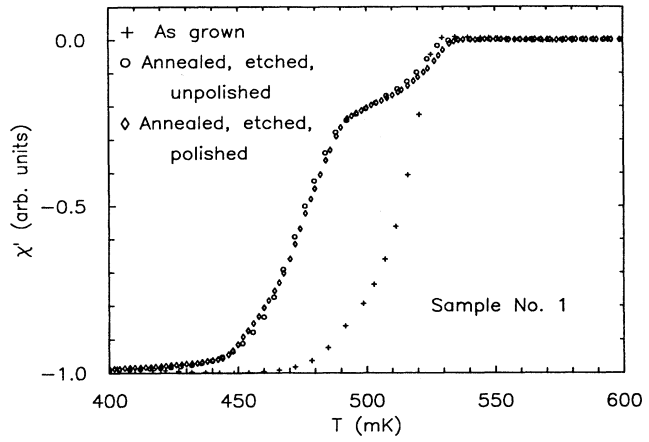

FIG. 6. Real part of the susceptibility, $\chi'(T)$, from mutual inductance (317 Hz) for single crystal no. 1 in the vicinity of T_c with $\mathbf{B}_{ac} \| c$ axis; "as grown" (+), annealed, etched, unpolished (○), annealed, etched, polished (◇). The change in the signal from T_{min} to T_c was normalized to -1. The double transition is observed only after annealing and etching. Polishing did not affect the onset of T_c significantly.

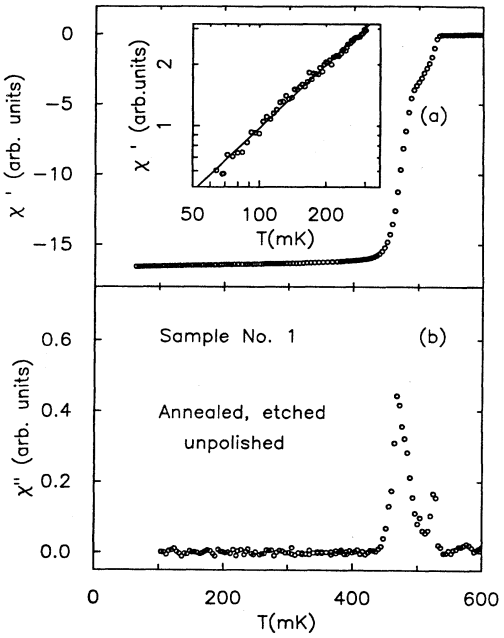

FIG. 7. $\chi'(T)$ and $\chi''(T)$ for single crystal no. 1 (etched, annealed, unpolished) with $\mathbf{B}_{ac} \| c$ axis. The kink near T_c is clearly observable. The inset is a log-log plot of the data for $T/T_c \leq 0.5$. The solid line represents the result of a linear fit and yields $\eta = 1.0 \pm 0.1$ [Eq. (2), Table I]. The same scale of arbitrary units were used for $\chi'(T)$ and $\chi''(T)$.

some volume of the sample was lost after each step of the surface treatment. To facilitate the comparison in Fig. 6, this total change in signal was normalized to -1. It is important to note that the double transition near T_c was only observable after annealing and etching. Furthermore, the onset of T_c was not significantly affected by the polishing process.

The results for sample no. 1 (etched, annealed, unpolished) over the entire temperature range are shown in Fig. 7. The double feature observed in $\chi'(T)$ [Fig. 7(a)] near T_c corresponds to a double peak in $\chi''(T)$ as shown in Figs. 7(b) and 8. The temperature difference between the two peaks, ΔT, was consistent with the double jump observed in the specific heat (Fig. 9). The inset of Fig. 7(a) shows a log-log plot of the results for $T/T_c \leq 0.5$. A linear least-squares fit indicates that the data fall on a straight line with a slope of $\eta = 1.0 \pm 0.1$, where η is defined in Eq. (2) and listed in Table I. The uncertainty in η represents one standard deviation.

The data for sample no. 1 (annealed, etched, and polished) are shown in Fig. 10. The kink in $\chi'(T)$ was still present near T_c, but the double peak in $\chi''(T)$ has almost disappeared [Figs. 8 and 10(b)]. The decrease in losses at T_c after polishing can be understood by a decrease in the volume where losses take place. The low-temperature results are shown in the inset of Fig. 10(a) on a log-log plot. The data fall on a straight line of slope $\eta = 1.0 \pm 0.1$ [Eq. (2), Table I].

The mutual inductance data presented in Figs. 6–10 were taken at 317 Hz. Similar measurements on the polished crystals were obtained at 47.3 Hz, 473 Hz, and 4.73 kHz. The double transition and the linear temperature dependence were independent of frequency over the investigated range.[32]

Previous measurements of the specific heat of a single crystal in magnetic fields parallel to the c axis showed the two jumps near T_c subsisting in fields up to 0.75 T, above which only one broad transition could be seen.[6] These results motivated a study of the kink in $\chi'(T)$, observed in sample no. 1, as a function of magnetic field. The dc field ($0 \leq B \leq 1.6$ T) was applied parallel to $\mathbf{B}_{ac}$ and to the c axis of the crystal. The resulting phase diagram is presented in Fig. 11, where the circles represent the first transition (T_{c1}) and the crosses correspond to the kink in

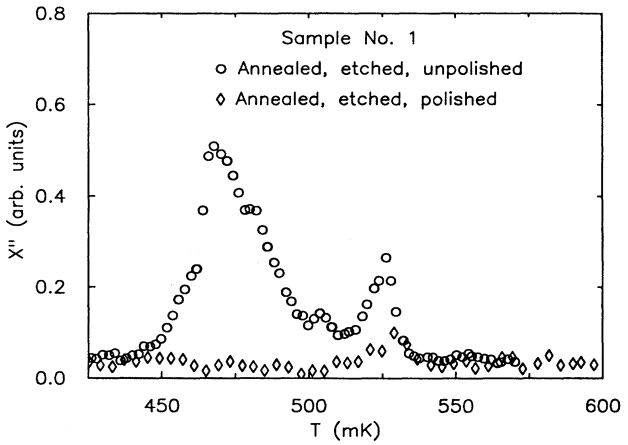

FIG. 8. The imaginary part of the susceptibility, $\chi''(T)$ taken at 317 Hz and with $\mathbf{B}_{ac} \| c$ axis for single crystal no. 1 before (○) and after (◇) polishing, in the vicinity of T_c.

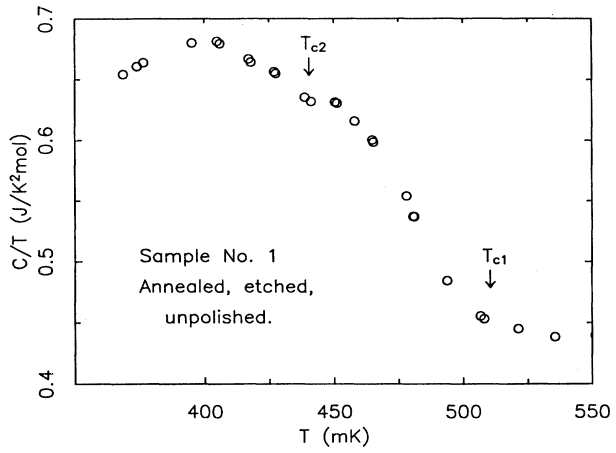

FIG. 9. The specific-heat data of sample no. 1 (annealed, etched, unpolished). The double transition is observable with a splitting, $\Delta T_c = T_{c1} - T_{c2}$, of about 60 mK. The peaks in $\chi''(T)$ for the unpolished sample are also 60 mK apart (Fig. 8).

$\chi'(T)$ at the lower transition (T_{c2}). The significance of these results are discussed at length in the next section.

A second interesting feature came out of the field measurements. For $B_{dc} \geq 1.2$ T, an upturn in $\chi'(T)$ was observable at the lowest temperatures (Fig. 12). Although the origin of such a paramagneticlike signal is unknown,

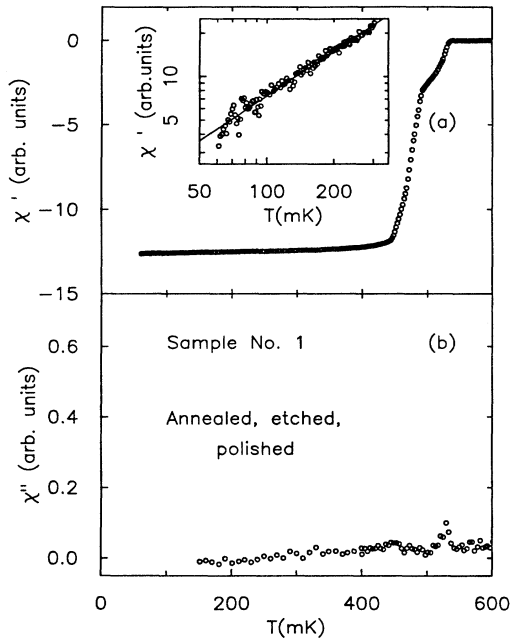

FIG. 10. $\chi'(T)$ and $\chi''(T)$ for single crystal no. 1 (annealed, etched, polished) with $\mathbf{B}_{ac} \| c$ axis. The kink near T_c is clearly observable in $\chi'(T)$. The inset shows a log-log plot of $\chi'(T)$ for $T/T_c \leq 0.5$. The solid line represents the result of a linear fit and yields $\eta = 1.0 \pm 0.1$ [Eq. (2), Table I]. The double peak in $\chi''(T)$ is diminished compared to before polishing (Fig. 8). The same scale of arbitrary units were used for $\chi'(T)$ and $\chi''(T)$.

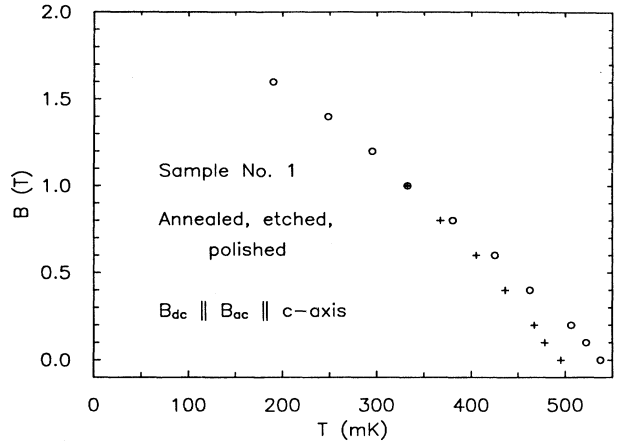

FIG. 11. The B-T phase diagram for single crystal no. 1 (annealed, etched, polished) constructed from the double transition in $\chi'(T)$, [T_{c1} (○), T_{c2} (+)] with $\mathbf{B}_{dc} \| \mathbf{B}_{ac} \| c$ axis.

a number of possibilities will be discussed in the next section.

The results for $\chi'(T)$ and $\chi''(T)$ on sample no. 2 (Table I) are presented in Fig. 13. In this unannealed single crystal, the double feature near T_c was not observable in either $\chi'(T)$ or $\chi''(T)$. Inductive and specific-heat measurements[47,48] by other groups have also established a single transition for this sample. The inset of Fig. 13(a) shows $\chi'(T)$ for $T/T_c \leq 0.5$ on a log-lot plot. The line is the result of a linear fit and indicates that the data fall on a straight line of slope $\eta = 2.0 \pm 0.2$ [Eq. (2), Table I]. This quadratic temperature dependence of $\lambda(T)$ is consistent with results previously reported on this sample.[14,18,47]

Figure 14 shows the results of $\chi'(T)$ and $\chi''(T)$ for sample no. 3 (Table I). The onset of the transition for this unannealed single crystal was observed at 450 mK, a significantly lower temperature compared to the other three samples. The data near T_c did not exhibit any kink in $\chi'(T)$ and showed only one peak in $\chi''(T)$. A log-log plot of $\chi'(T)$ for $T/T_c \leq 0.5$ is shown in the inset of Fig.

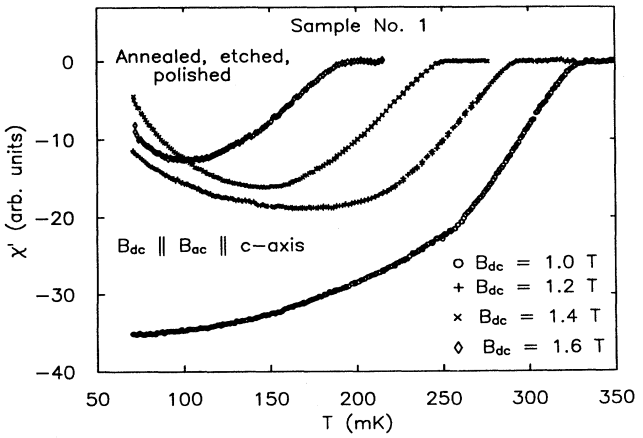

FIG. 12. $\chi'(T)$ for sample no. 1 (annealed, etched, polished) for $B_{dc} \geq 1$ T. An upturn is clearly observable for $B_{dc} \geq 1.2$ T.

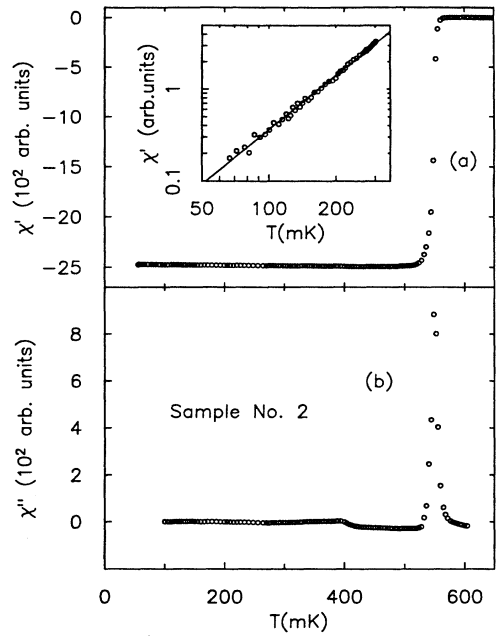

FIG. 13. $\chi'(T)$ and $\chi''(T)$ for sample no. 2 with $\mathbf{B}_{ac}\|c$ axis. There is no double feature near T_c in this unannealed single crystal. The inset shows a log-log plot of $\chi'(T)$ for $T/T_c \leq 0.5$. The solid line represents the result of a linear fit and yields $\eta=2.0\pm0.2$ [Eq. (2), Table I]. The same scale of arbitrary units were used for $\chi'(T)$ and $\chi''(T)$.

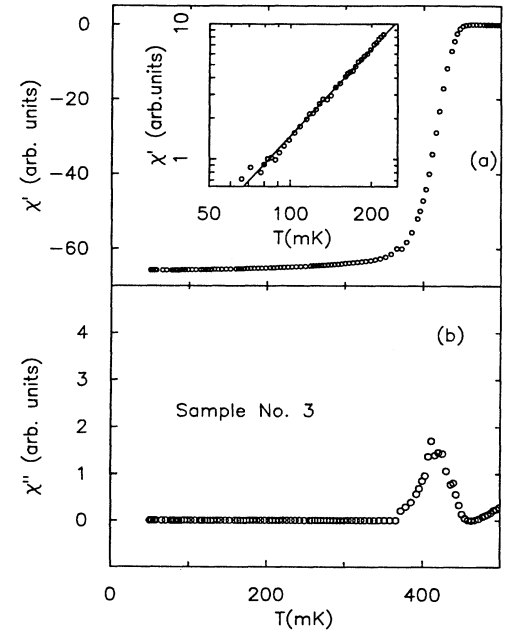

FIG. 14. $\chi'(T)$ and $\chi''(T)$ for sample no. 3 with $\mathbf{B}_{ac}\|c$ axis. There is no double feature near T_c in this unannealed single crystal. The inset shows a log-log plot of $\chi'(T)$ for $T/T_c \leq 0.5$. The solid line represents the result of a linear fit and yields $\eta=2.0\pm0.1$ [Eq. (2), Table I]. The same scale of arbitrary units were used for $\chi'(T)$ and $\chi''(T)$.

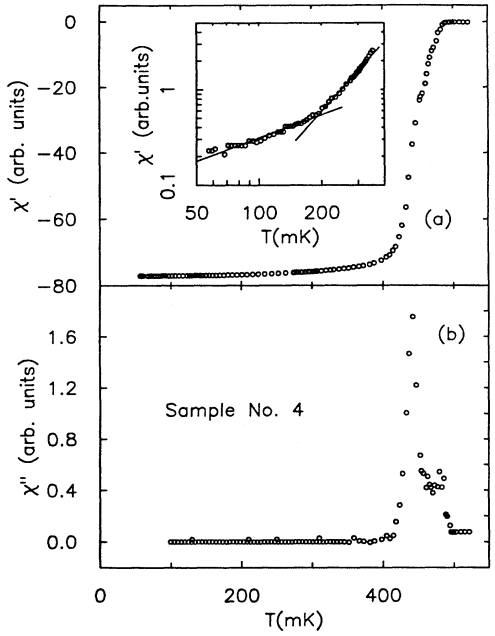

FIG. 15. $\chi'(T)$ and $\chi''(T)$ for the polycrystal sample (no. 4). The inset shows a log-log plot of $\chi'(T)$ for $T/T_c \leq 0.5$. The solid lines represent the results of a linear fits and yield $\eta=1.0\pm0.1$ [Eq. (2), Table I] for $T<200$ mK and $\eta=3.0\pm0.1$ for $200<T<300$ mK. The double feature near T_c is observable in $\chi'(T)$ and $\chi''(T)$, and the splitting is of the same order as that observed in specific-heat measurements (Ref. 4) and for sample no. 1 (Figs. 8–10). The same scale of arbitrary units were used for $\chi'(T)$ and $\chi''(T)$.

14(a). The solid line represents the result of a linear fit and yields $\eta=2.0\pm0.1$ [Eq. (2), Table I]. It is important to note here (with a detailed discussion to follow in the next section) that both sample nos. 2 and 3 exhibited a quadratic temperature dependence and a single transition at T_c.

The data for $\chi'(T)$ and $\chi''(T)$ on the polycrystalline sample, no. 4 (Table I), are shown in Fig. 15. The double feature in $\chi'(T)$ near T_c corresponds to two peaks in $\chi''(T)$, with a difference in temperature of about 60 mK. This splitting was equal to the one observed in the specific heat by Fisher *et al.*[4] and was on the same order as the one found for sample no. 1 (Figs. 8–10). The inset of Fig. 15(a) shows the low-temperature ($T/T_c \leq 0.5$) results for $\chi'(T)$ on a log-log plot. For temperatures below 200 mK, $\chi'(T)$ was linear in temperature [$\eta=1.0\pm0.1$, Eq. (2) and Table I], while between 200 and 300 mK, the data were best fitted to T^3 ($\eta=3.0\pm0.2$).

B. Resonant technique results

In this section, the data are presented by plotting the relative change in frequency, $\Delta f/f$, as a function of temperature, where $\Delta f/f=[f(T_{\min})-f(T)]/f(T_{\min})$. This expression is justified by Eq. (14) which shows that, for $T<T_c$, $\Delta f/f$ is proportional to the changes in the penetration depth. A comparison of the units from sam-

ple to sample is not possible since the inductors, and therefore the area A defined in Eq. (14), were different for each sample.

Figure 16 shows the relative change in frequency on single crystal no. 1 (annealed, etched, unpolished), for two different frequencies (3 and 16 MHz) and with $\mathbf{B}_{rf}\|c$ axis. Since the normal skin depth was larger for 3 MHz than for 16 MHz [Eq. (8)], $\Delta f/f$ at T_c was larger for 3 MHz than for 16 MHz. The inset of Fig. 16 shows a log-log plot for $T/T_c \leq 0.5$. The solid lines represent the result of linear fits and yield $\eta=2.5\pm0.1$ and $\eta=2.7\pm0.1$ for 3 and 16 MHz, respectively [Eq. (2), Table I].

Figure 17 shows the relative change in frequency on single crystal no. 1 (annealed, etched, polished), for two different frequencies (6 and 17 MHz) and with $\mathbf{B}_{rf}\|c$ axis. The low-temperature data for 6 MHz are shown in the inset of Fig. 17. On a log-log plot, the linear fit indicates that the data fall on a straight line of slope $\eta=3.7\pm0.2$. This result indicates that the polishing of the surface caused a significant change in the temperature dependence of $\lambda(T)$. This effect will be discussed in the next section.

The relative change of frequency as a function of temperature for single crystal no. 2 (Table I) at 5.6 MHz and with $\mathbf{B}_{rf}\|c$ axis is shown in Fig. 18. The inset of Fig. 18 shows a log-log plot for $T/T_c \leq 0.5$. The solid line represents the result of a linear fit and yields $\eta=2.4\pm0.2$ [Eq. (2), Table I].

The relative change of frequency as a function of temperature is shown in Fig. 19 for single crystal no. 3 (Table I) at 15 MHz. An important point to notice is the large ($\approx$50 mK) decrease in T_c onset when compared to the low-frequency results (Fig. 14). This decrease is due to self-heating of the sample near T_c arising from the presence of a significant quantity of quasiparticles near T_c. In addition, this effect is enhanced by the significant surface roughness (i.e., surface resistance) of this sample compared to others (Fig. 5). These effects are discussed in detail in the next section. Although some self-heating may still be present deep in the superconducting state, it should be dramatically reduced. Given this caveat, we have, for completeness, provided a log-log plot of the data for $T/T_c \leq 0.5$ (see inset of Fig. 19).

The data for sample no. 4 have already been published by Brown *et al.*[20] The authors reported a T^4 temperature dependence for $\Delta f/f$. The last two columns of Table I summarize the different temperature dependences for both techniques.

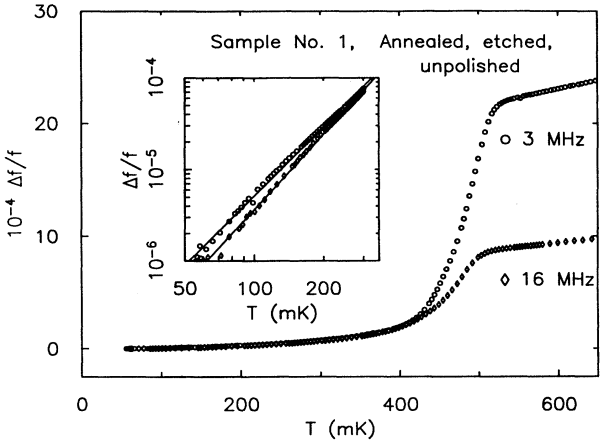

FIG. 16. The relative change in frequency $\Delta f/f=[f(T_{min})-f(T)]/f(T_{min})$, as a function of temperature for single crystal no. 1 (annealed, etched, unpolished) at 3 MHz (○) and 16 MHz (◊) and with $\mathbf{B}_{rf}\|c$ axis. The inset shows a log-log plot of $\Delta f/f(T)$ for $T/T_c \leq 0.5$. The solid line represents the result of a linear fit and yields $\eta=2.5\pm0.1$ for 3 MHz and 2.7 ± 0.1 for 16 MHz [Eq. (2), Table I].

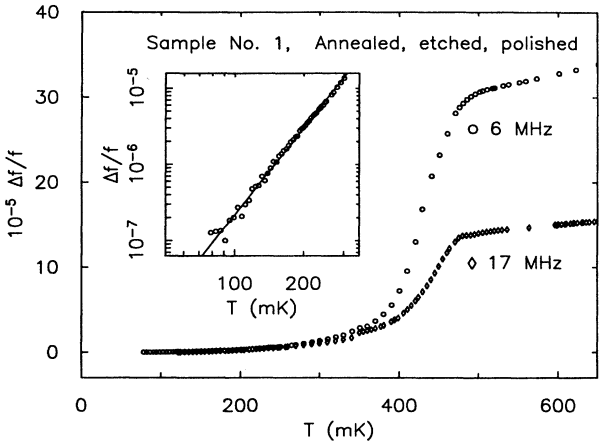

FIG. 17. The relative change in frequency $\Delta f/f=[f(T_{min})-f(T)]/f(T_{min})$ as a function of temperature for single crystal no. 1 (annealed, etched, and polished) at 6 MHz (○) and 17 MHz (◊) with $\mathbf{B}_{rf}\|c$ axis. The inset shows a log-log plot of $\Delta f/f(T)$ for $T/T_c \leq 0.5$. The solid line represents the result of a linear fit and yields $\eta=3.7\pm0.2$ [Eq. (2), Table I].

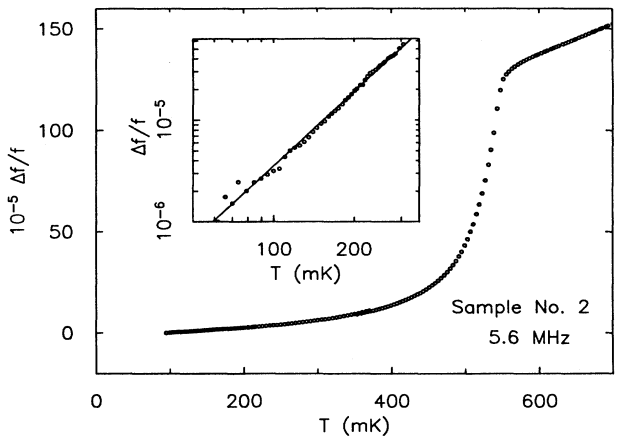

FIG. 18. The relative change in frequency $\Delta f/f=[f(T_{min})-f(T)]/f(T_{min})$ as a function of temperature for single crystal no. 2 at 5.6 MHz with $\mathbf{B}_{rf}\|c$ axis. The inset shows a log-log plot of $\Delta f/f(T)$ for $T/T_c \leq 0.5$. The solid line represents the result of a linear fit and yields $\eta=2.4\pm0.2$ [Eq. (2), Table I].

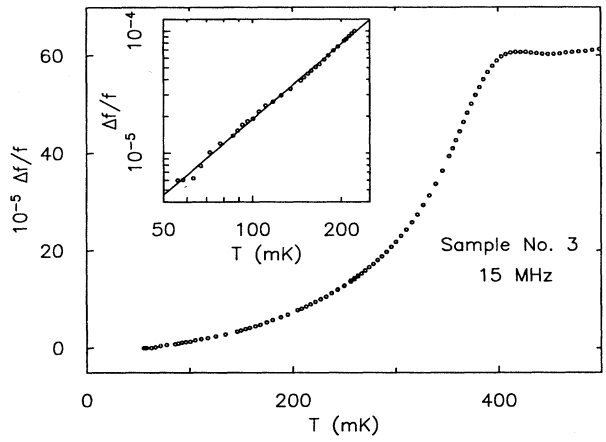

FIG. 19. The relative change in frequency $\Delta f/f=[f(T_{\min})-f(T)]/f(T_{\min})$ as a function of temperature for single crystal no. 3 at 15 MHz with $\mathbf{B}_{rf}\|c$ axis. The inset shows a log-log plot of $\Delta f/f(T)$ for $T/T_c \leq 0.5$. The solid line represents the result of a linear fit and yields $\eta=2.0\pm0.2$ [Eq. (2), Table I].

IV. DISCUSSION

A. Linear temperature dependence of $\lambda(T)$

From the low-frequency data on sample no. 1, Figs. 7(a) and 10(a), $\lambda(T)$ is linear in temperature for $T/T_c \leq 0.5$. Since the probing ac magnetic field is oriented parallel to the c axis of the crystal, the shielding currents run in the a-b plane. Therefore, the data suggest that the energy gap possesses a line of nodes in the a-b plane, and this arrangement is consistent with the polar state.[17] This identification is in agreement with thermal conductivity and ultrasonic attenuation experiments.[11,12,16] Furthermore, linearity in $\lambda(T)$ in the a-b plane agrees with μSR measurements by Broholm *et al.*,[21] where a hybrid state (i.e., line nodes in the basal plane and point nodes on the c axis) was proposed. However, questions have been raised about the validity of the μSR raw data analysis used to extract $\lambda(T)$.[43,54] Nevertheless, our work on sample no. 1 does not allow us to comment on the possibility of any gap nodes out of the a-b plane. One might think that insight into this point could be gained by considering the results on sample no. 4, Fig. 15. Gross *et al.*[17] have shown that, for the polar state, $\lambda(T)$ is linear in temperature for fields parallel to the c axis and $\lambda(T)\propto T^3$ for fields perpendicular to the c axis. In a polycrystal (such as our sample no. 4), where both orientations are present, one might expect to see $\lambda(T)\propto T$ dominate at low temperature and $\lambda(T)\propto T^3$ at higher temperatures. The data for sample no. 4, Fig. 15, *qualitatively* suggest that the temperature dependence is linear below 200 mK, but cubic between 200 and 300 mK. On the other hand, T^2 and T^4 contributions[17] might also arise if the hybrid state exists, and these effects may also be reflected in the data, Fig. 15. Therefore, our measurements cannot differentiate from these various possibilities. We are in a position to state that our results are consistent with line nodes in the basal plane, and further information about the gap structure out of the basal plane await additional experiments.

B. Quadratic temperature dependence of $\lambda(T)$

Our low-frequency data on sample no. 2, Fig. 13, have reproduced the quadratic temperature dependence of $\lambda(T)$ reported by Gross *et al.*[18] on the same specimen. This result suggests that the dc technique used by these authors is equivalent to our low-frequency mutual inductance method. It was in fact this quadratic temperature dependence which motivated Gross-Alltag *et al.*[14] to study the influence of impurities on the penetration depth. These authors suggested that $\lambda(T)\propto T^2$ could be explained by the presence of nonmagnetic impurities.

A quadratic temperature dependence was also observed for sample no. 3, Fig. 14. Another common feature between specimen nos. 2 and 3 is the single transition observed at T_c. It is interesting to note that neither sample was annealed. A connection between annealing and the presence of double transitions near T_c has already been reported[53] and is further emphasized by our results on sample no. 1. Before annealing, sample no. 1 did not show signs of double transitions, but after annealing, the double feature in $\chi'(T)$ was clearly observable (Fig. 6). The obvious conclusion from these results is that unannealed specimens possess a quadratic $\lambda(T)$. However, this interpretation is not supported by our work on sample no. 1 (unannealed),[32] where a quadratic temperature dependence is not observed but rather η [Eq. (2)] is closer to 1.

C. Double feature near T_c

From the low-frequency data on sample no. 1, Figs. 7 and 10, and on sample no. 4, Fig. 15, we also learn that the inductive response of the sample is sensitive to the double transition at T_c, observed by other measurements[4,6,7] and thought to be a signature of unconventional superconductivity in UPt_3. One might, at first, find this result surprising since it is usually thought that once superconductivity occurs, the supercurrents shield the bulk of the sample. This argument is valid for BCS-like superconductors, where the penetration depth is several orders of magnitude smaller that the coherence length, ξ. In UPt_3, $\lambda(T\rightarrow 0)\approx 1-2$ μm, which is much larger than ξ (≈ 100 Å).[55] We therefore expect our probing ac magnetic fields to be sensitive to the bulk superconducting state. Furthermore, the phase diagram constructed from our inductive measurements (Fig. 11) provides further evidence that the kinks in $\chi'(T)$ correspond to the transitions observed in experiments studying bulk properties (specific heat, thermal expansion, and sound velocity). Finally, we observed this effect in two different samples (nos. 1 and 4) which also showed double transitions in their specific heat, but we did not observe a kink in the samples that showed a single transition in their specific heat (sample nos. 2 and 3). It is noteworthy that this double feature near T_c has been observed in some other inductive measurements.[12,56]

D. High-frequency effects

1. *Temperature dependence of* $\lambda(T)$

For sample nos. 1, 2, and 4, $\lambda(T/T_c \leq 0.5)$ was different at high frequencies (≥ 3 MHz) compared to lower frequencies (≤ 4.7 kHz). This result clearly indicates that the discrepancy, discussed in the Introduction, between low and high frequencies was not simply related to the difference in samples used by the different groups. Our work clearly shows that these distinct results must come from either the differences in the methods used to measure $\lambda(T)$ (mutual inductance vs tunnel diode oscillator) or the intrinsic properties of UPt_3. In the following paragraphs, arguments are given against the former possibility. By default, the later interpretation is accepted and provides an additional evidence for unconventional superconductivity in UPt_3.

In Sec. II, the procedure for extracting $\lambda(T)$ from mutual inductance and tunnel diode oscillator measurements was described in detail. In the analysis, the important assumption was that the resistive part of the response goes to zero in the superconducting state. The mutual inductance technique allows this assumption to be checked by measuring $\chi''(T)$. In all our measurements, $\chi''(T)$ was essentially zero for temperatures below $T/T_c = 0.5$, the range from which the power laws were extracted. Therefore, our mutual inductance data correspond to the penetration depth, at least for $T/T_c \leq 0.5$. This assertion is supported by our results on sample no. 2 which agreed with the measurements by Gross-Alltag *et al.*[14] on the same sample using a dc magnetometer.

We now turn to the tunnel diode oscillator (TDO) technique, which does not directly measure the lossy contribution of the signal. First, it is important to recall the successful results on aluminum presented in Sec. II (Fig. 2). The aluminum data, taken using the TDO method, were well fitted by the BCS prediction for a type-I superconductor of $\lambda(T)$, given by Eq. (15). Furthermore, T_c was within 5 mK of the T_c observed with the mutual inductance method, indicating negligible self-heating from the resistive part of the signal. These results, in addition to the work of other workers with TDO techniques,[39,40] justify the use of the TDO method to measure $\lambda(T)$, at least in BCS-like superconductors. However, one might argue that, in superconductors possessing nodes in their energy gap structure, the density of normal electrons does not fall to zero as quickly as in a superconductor with a full gap around the Fermi surface. This assertion is discussed in the next paragraph, and in the context of our results for UPt_3.

In Fig. 20, the data on sample no. 2, in the vicinity of T_c, for both low and high frequencies are shown. In order to facilitate the comparison, the data was normalized so that the total change in signal between T_c and T_{min} is unity for both sets of data. Although T_c is nominally the same for both runs, a broadening of the transition was clearly observable for the rf measurement. A large broadening in addition to a shift in T_c was also present for sample no. 3 as can be seen by comparing Figs. 14 and 19. To understand this effect, let us go back to Eq. (14),

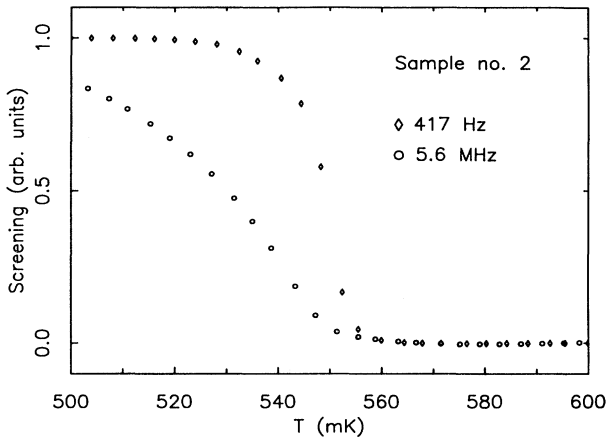

FIG. 20. The real part of the susceptibility, $\chi'(T)$ from mutual inductance (417 Hz) ($\Diamond$) and the relative change in frequency ($\circ$) from TDO measurements (5.6 MHz) as a function of temperature in the vicinity of T_c for single crystal no. 2. The change of the signals from T_{min} to T_c has been normalized to unity to facilitate the comparison. A slight broadening of the transition is observable for the high-frequency data.

where we asserted that, below T_c, $\Delta f/f$ was proportional to $\Delta\lambda$. In other words, the surface impedance consists completely of a reactance contribution and no resistive component. Pippard[57] has shown that this assertion is in general true except near the critical temperature where the presence of normal electrons introduces some resistance to the surface impedance. This resistive contribution gives the measured $\lambda(T)$ a weaker temperature dependence than the actual $\lambda(T)$, and as a consequence, the transition is broadened. This effect has already been discussed in relation to TDO inductive measurements on UPt_3 by Gannon *et al.*[19] In superconductors with finite gaps, such as Al, this effect is small because the density of quasiparticles quickly drops below T_c. In UPt_3, however, if we assume that the gap possesses nodes, the decrease of the density of quasiparticles, and of the surface resistance, R_s, is much slower. In fact, surface resistance in UPt_3 has been studied as a function of frequency by Grimes, Adams, and Bucher.[58] In their results, a rapid increase of R_s was seen with increasing frequency. This effect is probably also responsible for "washing out" the double feature at T_c for the high-frequency data on sample nos. 1 (Figs. 16 and 17) and 4 (Ref. 20). In order to determine precisely the temperature below which this effect becomes negligible, one would have to measure the *rf surface* resistivity. This quantity is likely to be different from sample to sample given their different surface imperfections. It is likely that well-polished samples exhibit the lowest surface resistivity at rf frequencies. In fact, Grimes, Adams, and Bucher[58] reported a surface resistance at 10 MHz and at 0.38 K that was only 1% of R_s at 0.7 K for their polished sample. We, therefore, do not believe that surface resistance effects are significant for well-polished samples of low residual resistivity, ρ_0, such as sample no. 1 of our study, which was polished and possessed a relatively low value for ρ_0.[32]

Finally, consider our polished sample no. 1. At rf frequencies, this specimen exhibited temperature dependences close to T^4 (Fig. 17). The only theoretical effort to reconcile these measurements with the linear dependence, obtained from the mutual inductance data (low frequencies), has been proposed by Putikka, Hirschfeld, and Wölfle[28] and Hirschfeld *et al.*[29] Unfortunately, the input assumptions to their analysis do not fully apply to our experimental conditions. For example, they predicted a frequency dependence in the clean limit, i.e., anomalous skin effect regime, or near the crossover $\lambda(T\rightarrow 0)\leq l$, where l is the mean free path ($l\approx 2000$ Å in UPt_3). Since neither one of these conditions applied to our samples [$\lambda(T\rightarrow 0)\approx 20\,000$ Å], the answer to the frequency dependence in UPt_3 remains to be given.

Finally, in an effort to search for a possible crossover from one frequency regime to the other, we have measured $\chi'(T=80$ mK) using the mutual inductance technique as a function of frequency from 37 Hz to 5 kHz.[32] We did not observe any crossover within the frequency space spanned. For future work, this type of measurement should be conducted between 5 kHz and 5 MHz.

2. *Peak around T_c in the rf measurements*

For sample nos. 3 and 4, a peak is observed around T_c for the rf measurements (Fig. 19 and Ref. 20), while this feature is not present for sample nos. 1 and 2 (Figs. 16–18). In this subsection, we discuss the nature of this peak, and argue that it is related to the size of the skin depth at T_c, $\delta(T_c)$ defined in Eq. (8), relative to the sample radius, and to the magnitude of the penetration depth, $\lambda(T)$, just below T_c.

Such peaks have already been reported for conventional superconductors, such as Ta (type I) and Nb (type II), and have been explained in terms of a crossover between the divergent penetration depth and the finite skin depth at T_c.[40,59] On the other hand, rf measurements on Sn and Al did not reveal any feature around T_c.[38,60] Furthermore, the effect was also observed in rf measurements of UPt_3 by Gannon *et al.*[19] who reported a broad peak around T_c for their 6.3- and 10-MHz data. In Fig. 21, our results for the rf measurements on sample no. 1 (annealed, etched, polished) are shown for two different frequencies. The 6-MHz data, also shown in Fig. 17, do not exhibit any feature near T_c, but the 33-MHz data, for the same sample, clearly do. This result suggests that the appearance of the peak is not sample dependent but is likely to be related to the size of the skin depth at T_c, which decreases with frequency [Eq. (8)], relative to the sample size.

Just below T_c, the penetration depth diverges, so that the magnetic field penetrates most of the sample. Above T_c, the skin depth determines the amount of field penetration. At low enough frequencies, and for small samples, $\delta(T_c)$ may become equal or greater than the sample size. In this case, the field penetrates most of the sample above *and* below T_c, and no peak is observed. At higher frequencies, $\delta(T_c)$ may become much smaller than the radius of the sample, so that the flux through the sample increases as the temperature drops below T_c,

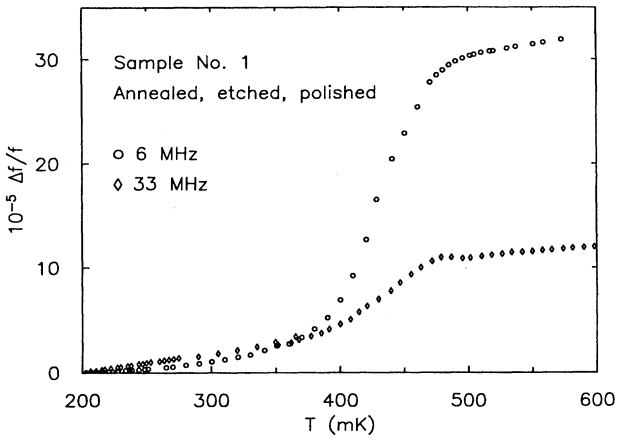

FIG. 21. The relative change in frequency $\Delta f/f=[f(T_{\min})-f(T)]/f(T_{\min})$ as a function of temperature for single crystal no. 1 (annealed, etched, and polished) at 6 MHz (○) and 33 MHz (◊) with $\mathbf{B}_{rf}\|c$ axis. A peak around T_c is observable only for the 33-MHz data.

causing a peak in the inductive response. The radius of sample no. 1 is $r_s=0.2$ mm, and we estimate $\delta(T_c$, 3 MHz$)\approx 50$ μm, so that a small peak would be observable with enough sensitivity. At 33 MHz, with $\delta(T_c$, 33 MHz$)\approx 10$ μm, the effect becomes more significant and observable in our measurements.

E. Upturn in $\chi'(T)$ for $B_{dc}\geq 1.2$ T

In this subsection, we discuss the upturn of $\chi'(T)$ observed below 200 mK, in sample no. 1 (annealed, etched, polished), and for fields greater than 1 T. The traces are shown in Fig. 12 and represent the only inductive results ever reported on superconducting UPt_3 for fields above 1 T. These results were surprising since one would expect a monotonic decrease in $\chi'(T)$ as $T\rightarrow 0$, and a decrease in the total change in signal, $\Delta\chi'(T)$, between T_c and the minimum temperature, $T_{\min}$, with increasing magnetic field since $\Delta\chi'(T)$ is a measure of the amount of flux in the sample. We recall that the data were taken in zero-field-cooled conditions (there are no field-cooled data available) and with a probing frequency of 317 Hz (the frequency dependence was not investigated). Furthermore, we note that $\chi''(T)$ was temperature independent below T_c.

To allow the analysis of the upturn in $\chi'(T)$, the superconducting transition was subtracted from the raw data and plotted in Fig. 22, for $B_{dc}=1.4$ T. More specifically, the temperature dependence of the signal corresponding to the superconducting transition was assumed to be quadratic below T_c. This assumption was supported by the quadratic dependence of $\chi'(T)$ observed for the $B_{dc}=1$ T.

A possible interpretation for the upturn is that it arises from the background temperature dependence of the coil and of the copper wires on which the sample was GE varnished. However, this possibility is not supported by the response of a temperature sweep, taken at $B_{dc}=2$ T, of

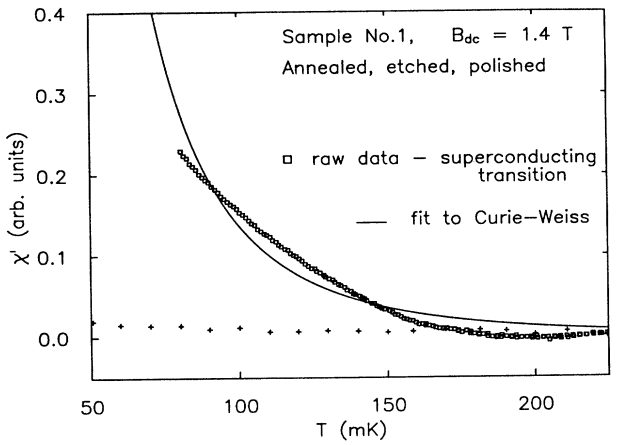

FIG. 22. The upturn in $\chi'(T)$ for $B_{dc}=1.4$ T (□). The superconducting transition was subtracted from the raw data (see text). The line represents an attempt to fit the upturn to a Curie-Weiss law. The temperature dependence of the background (coil and copper wires) for $B_{dc}=2$ T is shown (+).

the coil in the absence of the specimen but with similar copper wires used for the thermal anchoring of sample no. 1. The data are shown in Fig. 22, and indicate that the background temperature dependence is negligible compared to the signal observed in the presence of the sample. The upturn is, therefore, intrinsic to sample no. 1.

A second possibility may be the presence of magnetic impurities, which, at low temperatures and high magnetic fields can provide a paramagnetic signal. However, this explanation cannot account for the sudden appearance of the upturn for $B_{dc} \geq 1.2$ T, and the complete absence of any paramagnetic signal in the 1 T sweep (Fig. 12). Furthermore, if impurities caused the paramagnetic signal, one would expect the onset temperature of this upturn to increase with field. This prediction is in conflict with the observation of a decrease in temperature with increasing field (Fig. 12). In addition, the temperature dependence of the magnetic susceptibility arising from impurities might follow a Curie-Weiss law, i.e., $\chi'(T) \sim 1/(T-\Theta)$, where Θ is the Curie-Weiss temperature. In Fig. 22, an attempt to fit the data to such temperature dependence is shown, and indicates that the upturn does not follow a Curie-Weiss law.

A third possible interpretation is that the upturn is an intrinsic feature of the superconducting state of UPt_3. The B-T phase diagram of UPt_3, for fields parallel to the c axis,[7] indicates the presence of a transition line around 1.2 T for temperatures below 200 mK. Schenstrom *et al.*[61] have suggested that this transition line corresponds to a structural transition, known as H_{FL}, in which the symmetry of the flux lattice (FL) changes. From this phase diagram, it is clear that, for our measurements below 200 mK, the sample is in one phase for $B_{dc} \geq 1.2$ T, and in a different phase for $B_{dc} < 1.2$ T, explaining the fact that we obtain different responses above and below 1.2 T. However, within this interpretation, the low-temperature increase, observed in our measurements for fields above 1.2 T, would indicate an increase in total flux penetrating the sample as the specimen is *cooled* through the higher field phase. The reason for such an increase of flux in the low-temperature–high-field phase as the temperature decreases is not clear.

A fourth explanation for the upturn in $\chi'(T)$ is related to flux motion inside the sample. As mentioned above, the sample was first cooled to T_{min} in the Earth's field, the dc magnetic field was then slowly increased (0.03 T/min) to the set point, so as to not generate any significant heating, and subsequently (within 15 min) the temperature was increased at a rate of about 0.75 mK/min. It is possible that the equilibrium distribution of vortices was never established at the lowest temperatures, and that the upturn corresponds to a time relaxation toward the equilibrium configuration. This assertion is supported by the work of Pollini *et al.*[62] who reported magnetization measurements on UPt_3 and suggested the presence of strong flux motion, even at mK temperatures (7 mK). A simple experiment that could shed light on this issue is to measure χ' as a function of time, at fixed field and fixed temperature. Although we consider this fourth possibility to be the most plausible explanation of the effect, future investigations will be needed to elucidate this phenomenon.

V. SUMMARY

The first important conclusion drawn from our low-frequency measurements is that the temperature dependence of the penetration depth of UPt_3 is linear for currents flowing in the a-b plane and for $T/T_c \leq 0.5$. This finding was consistent for all annealed, high-quality samples, showing a double transition in the vicinity of T_c. This result strongly suggests that the energy gap possesses lines of nodes in the basal plane.

The second conclusion is that the double feature near T_c, observed in our low-frequency inductive measurements, corresponds to the same double transition observed with bulk measurements such as specific heat, thermal expansion, and sound velocity-attenuation. This conclusion contradicts the statement, often reported, that this feature is an extrinsic property of UPt_3.

The third conclusion is the fact that the temperature dependence of the penetration depth in UPt_3 is frequency dependent, even for frequencies 2 orders of magnitude less than the energy gap frequency. We believe that this frequency dependence is an intrinsic property of the superconductivity in UPt_3 and arises from its unconventionality.

ACKNOWLEDGMENTS

Throughout the course of this work, we have benefited from enlightening conversations and correspondence with many colleagues, including A. de Visser, A Garg, W. P. Halperin, P. J. Hirschfeld, J. B. Ketterson, E. A. Knetsch, Z. Koziol, S. Lin, J. A. Sauls, F. Sharifi (who kindly provided us with the use of his scanning electron microscope), B. S. Shivaram, G. R. Stewart, and S. K.

Yip. We gratefully acknowledge participation in the data acquisition, at various times during the course of this work, from J. Bremer, E. A. Knetsch, J. P. Koster, S. Lin, A. Rafanello, and C. M. C. M. van Woerkens. Several aspects of this work have used the facilities of the UF Major Analytical Instrumentation Center (MAIC). This work was supported, in part, by the National Science Foundation [DMR-9200671 (M.W.M.), DMR-9400755 (B.A.)]. The work at Los Alamos National Laboratory is conducted under the auspices of the Department of Energy. One of us (M.W.M.) gratefully acknowledges the hospitality of Northwestern University and the NU MRC UPt_3 Thrust Group during the preparation of this manuscript.

---

*Electronic address: Meisel@phys.ufl.edu

†Present address: Department of Physics and the National High Magnetic Field Laboratory, Florida State University, 1800 East Paul Dirac Drive, Box 4005, Tallahassee, FL 32306-4005.

[1]G. R. Stewart, Z. Fisk, J. O. Willis, and J. L. Smith, Phys. Rev. Lett. **52**, 679 (1984).

[2]For experimental reviews, see, for example, G. R. Stewart, Rev. Mod. Phys. **56**, 755 (1984); Z. Fisk and G. Aeppli, Science **260**, 38 (1993); H. v. Löhneysen, Physica B **197**, 551 (1994).

[3]For theoretical reviews, see, for example, M. Sigrist and K. Ueda, Rev. Mod. Phys. **63**, 239 (1991); R. Joynt, J. Magn. Magn. Mater. **108**, 31 (1992); J. A. Sauls, J. Low Temp. Phys. **95**, 153 (1994); Adv. Phys. **43**, 113 (1994).

[4]R. A. Fisher, S. Kim, B. F. Woodfield, N. E. Phillips, L. Taillefer, K. Hasselbach, J. Flouquet, A. L. Giorgi, and J. L. Smith, Phys. Rev. Lett. **62**, 328 (1989).

[5]B. S. Shivaram, T. F. Rosenbaum, and D. G. Hinks, Phys. Rev. Lett. **57**, 1259 (1986); B. S. Shivaram, J. J. Gannon, Jr., and D. G. Hinks, Phys. Rev. Lett. **63**, 1723 (1989).

[6]K. Hasselbach, L. Taillefer, and J. Flouquet, Phys. Rev. Lett. **63**, 93 (1989); K. Hasselbach, A. Lacerda, K. Behnia, L. Taillefer, J. Flouquet, and A. de Visser, J. Low Temp. Phys. **81**, 299 (1990).

[7]S. Adenwalla, S. W. Lin, Q. Z. Ran, Z. Zhao, J. B. Ketterson, J. A. Sauls, L. Taillefer, D. J. Hinks, M. Levy, and Bimal K. Sarma, Phys. Rev. Lett. **65**, 2298 (1990).

[8]S. W. Lin, Ph.D. dissertation, University of Wisconsin, Milwaukee, 1993.

[9]T. Trappman, H. v. Löhneysen, and L. Taillefer, Phys. Rev. B **43**, 13 714 (1991).

[10]H. v. Löhneysen, T. Trappman, and L. Taillefer, J. Magn. Magn. Mater. **108**, 49 (1992).

[11]D. J. Bishop, C. M. Varma, B. Batlogg, E. Bucher, Z. Fisk, and J. L. Smith, Phys. Rev. Lett. **53**, 1009 (1984).

[12]A. Sulpice, P. Gandit, J. Chaussy, J. Flouquet, D. Jaccard, P. Lejay, and J. L. Tholence, J. Low. Temp. Phys. **62**, 93 (1986).

[13]B. S. Shivaram, Y. H. Jeong, T. F. Rosenbaum, and D. G. Hinks, Phys. Rev. Lett. **56**, 1078 (1986).

[14]F. Goss-Alltag, B. S. Chandrasekhar, D. Einzel, P. J. Hirschfeld, and K. Andres, Z. Phys. B **84**, 243 (1991).

[15]C. Jin, D. M. Lee, S.-W. Lin, Bimal K. Sarma, and D. G. Hinks, J. Low Temp. Phys. **89**, 557 (1992).

[16]K. Behnia, D. Jaccard, L. Taillefer, J. Flouquet, and K. Maki, J. Magn. Magn. Mater. **108**, 133 (1992).

[17]F. Gross, B. S. Chandrasekar, D. Einzel, K. Andres, P. J. Hirschfeld, H. R. Ott, J. Beuers, Z. Fisk, and J. L. Smith, Z. Phys. B **64**, 175 (1986).

[18]F. Gross, B. S. Chandrasekhar, K. Andres, U. Rauchschwalbe, E. Bucher, and B. Lüthi, Physica C **153-155**, 439 (1988).

[19]J. J. Gannon, Jr., B. S. Shivaram, and D. G. Hinks, Europhys. Lett. **13**, 459 (1990).

[20]S. E. Brown, H. Li, M. W. Meisel, J. L. Smith, A. L. Giorgi, and J. D. Thompson, Physica B **165&166**, 377 (1990).

[21]C. Broholm, G. Aeppli, R. N. Kleiman, D. R. Harshman, D. J. Bishop, E. Bucher, D. Ll. Williams, E. J. Ansaldo, and R. H. Heffner, Phys. Rev. Lett. **65**, 2062 (1990).

[22]Z. Koziol, Ph.D. dissertation, University of Amsterdam, Amsterdam, The Netherlands, 1994.

[23]P. J. C. Signore, J. P. Koster, E. A. Knetsch, C. M. C. M. van Woerkens, M. W. Meisel, S. E. Brown, and Z. Fisk, Phys. Rev. B **45**, 10 151 (1992).

[24]P. J. C. Signore, M. W. Meisel, S. E. Brown, and Z. Fisk, Physica B **199&200**, 157 (1994).

[25]W. N. Hardy, D. A. Bonn, Ruixing Liang, and Kuan Zhang, Phys. Rev. Lett. **70**, 3999 (1993).

[26]D. Achkir, M. Poirer, D. A. Bonn, Ruixing Lang, and W. N. Hardy, Phys. Rev. B **48**, 13 184 (1993).

[27]Zhengxiang Ma, R. C. Taber, L. W. Lombardo, A. Kapitulnik, M. R. Beasley, P. Merchant, C. B. Eom, S. Y. Hou, and Julia M. Phillips, Phys. Rev. Lett. **71**, 781 (1993).

[28]W. O. Putikka, P. J. Hirschfeld, and P. Wölfle, Phys. Rev. B **41**, 7285 (1990).

[29]P. J. Hirschfeld, W. O. Putika, P. Wölfle, and Y. Campbell, J. Low Temp. Phys. **88**, 395 (1992).

[30]R. N. Kleiman, D. J. Bishop, H. R. Ott, Z. Fisk, and J. L. Smith, Phys. Rev. Lett. **64**, 1975 (1990).

[31]A. de Visser, N. H. van Dijk, K. Bakker, J. J. M. Franse, A. Lacerda, J. Flouquet, Z. Fisk, and J. L. Smith, Phys. Rev. B **45**, 2962 (1992).

[32]P. J. C. Signore, Ph.D. dissertation, University of Florida, Gainesville, 1994.

[33]L. D. Landau and E. M. Lifshitz, *Electrodynamics of Continuous Media* (Pergamon, New York, 1984).

[34]E. Maxwell and M. Strongin, Phys. Rev. Lett. **10**, 212 (1963).

[35]A. F. Khoder, Phys. Lett. **94A**, 378 (1983).

[36]R. A. Hein, Phys. Rev. B **33**, 7539 (1986).

[37]Morton Thiokol Inc., 152 Andover St., Danvers, MA 01923.

[38]W. L. McLean, Proc. Phys. Soc. **79**, 572 (1962).

[39]P. M. Tedrow, G. Faraci, and R. Meservey, Phys. Rev. B **4**, 74 (1971).

[40]C. Varmazis and M. Strongin, Phys. Rev. B **10**, 1885 (1974); C. Varmazis, J. R. Hook, D. J. Sandiford, and M. Strongin, *ibid.* **11**, 3354 (1975).

[41]Model BD-5 from Germanium Power Devices, P.O. Box 3065, 300 Brickstone Square, Shawsheen Village Station, Andover, MA 01180-0865.

[42]W. F. Chow, *Principles of Tunnel Diode Circuits* (Wiley, New York, 1964).

[43]G. M. Luke, L. P. Le, B. J. Sternlieb, W. D. Wu, Y. J. Uemura, J. H. Brewer, R. Kadono, R. F. Kiefl, S. R. Kreitzman, T. M. Riseman, Y. Dalichaouch, B. W. Lee, M. B. Maple, C. L. Seaman, P. E. Armstrong, R. W. Ellis, Z. Fisk, and J. L. Smith, Phys. Lett. **157**, 173 (1991).

[44]A. K. Raychaudhuri, C. Egloff, and L. Rinderer, J. Low Temp. Phys. **53**, 513 (1983).
[45]T. van Duzer and C. W. Turner, *Principles of Superconducting Devices and Circuits* (Elsevier, New York, 1981).
[46]B. W. Roberts, J. Phys. Chem. Data **5**, 581 (1976).
[47]E. A. Schuberth, G. Hofmann, F. Gross, K. Andres, and J. Hufnagl, Europhys. Lett. **11**, 249 (1990).
[48]B. Ellman, J. Yang, T. F. Rosenbaum, and E. Bucher, Phys. Rev. Lett. **64**, 1569 (1990).
[49]E. A. Schuberth (unpublished).
[50]A. A. Menovsky and J. J. M. Franse, J. Cryst. Growth **65**, 286 (1983).
[51]E. A. Knetsch and A. de Visser (private communication).
[52]A. de Visser and Z. Koziol (private communication).
[53]T. Vorenkamp, Z. Tarnawski, H. P. van der Meulen, K. Kadowaki, V. J. M. Meulenbroek, A. A. Menovsky, and J. J. M. Franse, Physica B **163**, 564 (1990).
[54]G. M. Luke, A. Keren, L. P. Le, W. D. Wu, Y. J. Uemura, D. A. Bonn, L. Taillefer, and J. D. Garrett, Phys. Rev. Lett. **71**, 1466 (1993).
[55]J. W. Chen, S. E. Lambert, M. B. Maple, Z. Fisk, J. L. Smith, G. R. Stewart, and J. O. Willis, Phys. Rev. B **30**, 1583 (1984).
[56]G. Bruls, D. Weber, B. Wolf, P. Thalmeier, B. Lüthi, A. de Visser, and A. Menovsky, Phys. Rev. Lett. **65**, 2294 (1990).
[57]A. B. Pippard, Proc. R. Soc. London Ser. A **191**, 399 (1947).
[58]C. C. Grimes, G. Adams, and E. Bucher, Phys. Rev. B **44**, 4631 (1991).
[59]C. Varmazis, Y. Imry, and M. Strongin, Phys. Rev. B **13**, 2880 (1976).
[60]A. L. Schawlow and G. E. Devlin, Phys. Rev. **113**, 120 (1959).
[61]A. Schenstrom, M.-F. Xu, Y. Hong, D. Bein, M. Levy, Bimal Sarma, S. Adenwalla, Z. Zhao, T. Tokuyasu, D. W. Hess, J. B. Ketterson, J. A. Sauls, and D. G. Hinks, Phys. Rev. Lett. **62**, 332 (1989).
[62]A. Pollini, A. C. Mota, P. Visani, G. Juri, and J. J. M. Franse, Physica B **165&166**, 365 (1990); A. Pollini, A. C. Mota, P. Visani, R. Pittini, G. Juni, T. Teruzzi, and J. J. M. Franse, Physica C **185-189**, 2625 (1991).

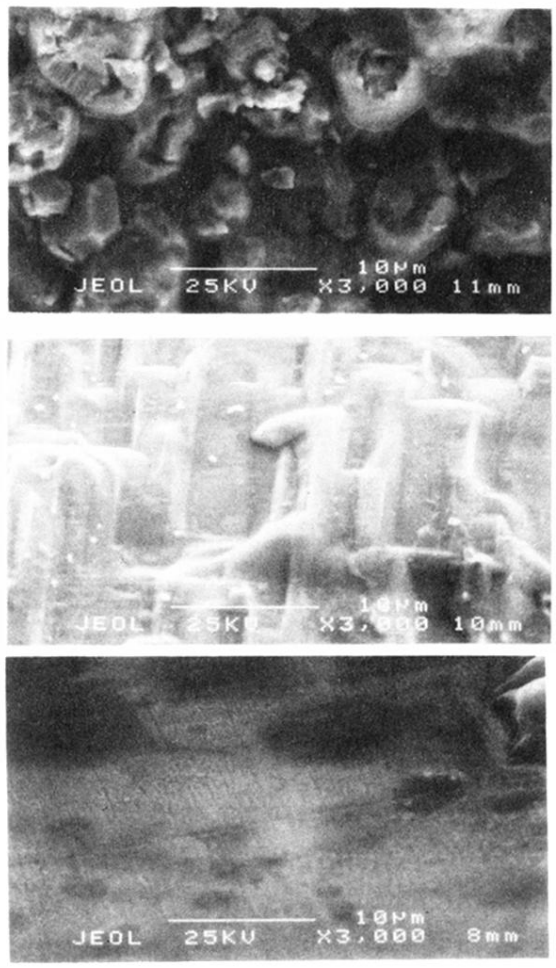

(a)

(b)

(c)

FIG. 3. SEM pictures ($\times 3000$ magnification) of the surface of single crystal no. 1 (Table I). (a) As grown; (b) annealed, etched, unpolished; (c) annealed, etched, polished. The length scale of the imperfections improve from about 2 μm to less than 0.5 μm.

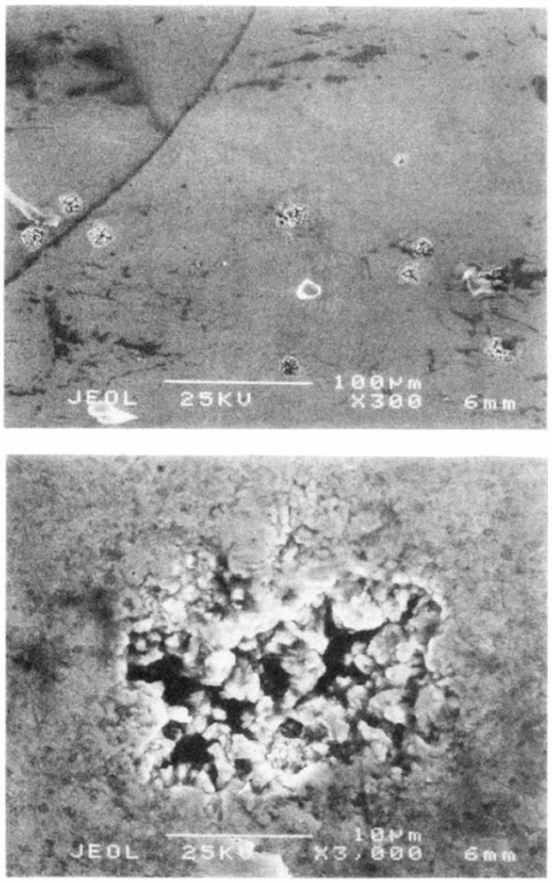

(a)

(b)

FIG. 4. 4 SEM pictures of the surface of single crystal no. 2 (Table I). (a) $\times 300$ magnification, the length scale of the imperfections is less than 2 μm, except to a few cracks (upper left corner) and scattered "pin holes" occupying less than 5% of the total surface area. (b) $\times 3000$ magnification, focusing on one of the "pin holes."

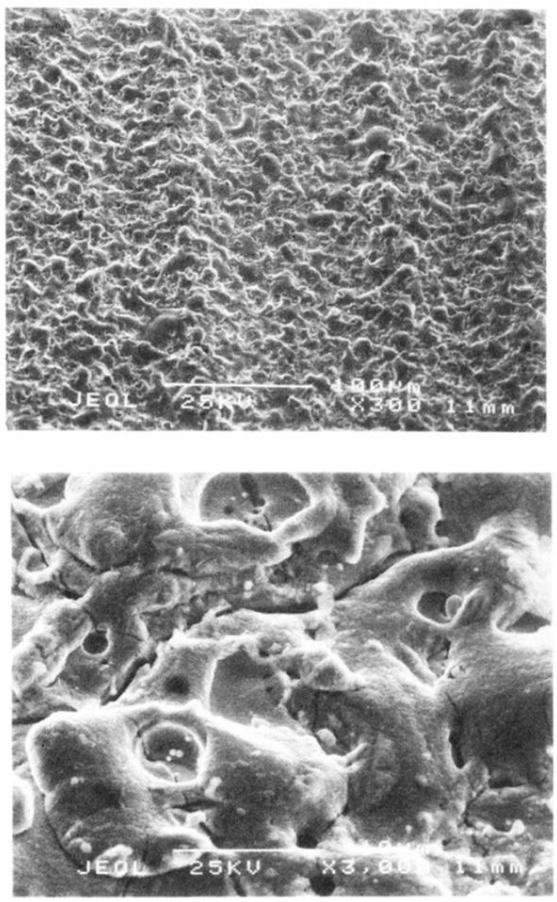

FIG. 5. SEM pictures of a specimen originating from the same batch as sample no. 3 (Table I). (a) $\times 300$ magnification. (b) $\times 3000$ magnification. Imperfections possessing a length scale between 1 and 10 μm cover the entire surface.